CHARACTERISATION ON PLA - SILK FIBRE COMPOSITES FOR PROSTHETIC APPLICATIONS

H.Y. Cheung*, J. Dean, B. Stearn and T.W. Clyne[1]

[1]*Department of Materials Science and Metallurgy, University of Cambridge, Pembroke Street, Cambridge, United Kingdom CB2 3QZ*
**Khyc2@cam.ac.uk*

Keywords: silkworm silk fibre, poly(lactic acid), mechanical property, material characterisation

Abstract
Composite material was made by blending of silk fibres with poly(lactic acid) (PLA) with injection moulding technique. The resultant composite contained about 5-15 vol% of fibre, with either planar random or unidirectional fibre orientations. Mechanical properties of neat PLA and silk/PLA composite were examined by tensile and ultrasonic resonance tests, and was confirmed via Izod fracture energy measurements that the presence of these fibres substantially enhanced the mechanical properties of the PLA matrix. Microscopic imaging examined fibre dispersion and orientation, as well as the fracture mechanism of silk/PLA composite. Investigations were also made into the chemical characterisation by FTIR of this type of bio-engineering composite.

1 Introduction
Recent advances in natural fibre development, genetic engineering, and composite science offer significant opportunities for improved materials from renewable resources with enhanced support for global sustainability [1]. There is current interest [2-4] in the development of composites containing natural fibres, especially silk fibres (from silkworms), for biomedical applications. Fibres of this type have been in use for various applications over an extended period. For example, they are widely used as suture material for healing of wounds. Composites consist of biodegradable polymer as matrix and bio-fibres (natural fibres) as reinforcing elements which are generally low cost, low density, high toughness, acceptable specific strength properties, good thermal properties, ease of separation, enhanced energy recovery and biodegradability. Synthetic biodegradable polymers like PLA, which is derived from renewable resources, are generally degraded by simple hydrolysis and have a promising advantage over natural polymers for implant development as their material properties are more predictable and reproducible [5]. They can be easily modified or altered to achieve desirable mechanical and degradation characteristics. Natural fibres are chosen as reinforcements since they can reduce the chance of tool wear when processing and dermal and respiratory irritation [6]. Conversely, these fibres are usually small in cross-sections and cannot be directly used in engineering applications; they are embedded in matrix materials to form bio-composites. The matrix serves as a binder to bind the fibres together and transfer loads to the fibres. The reinforcement of the natural fibres can at the same time enhancing the material properties of the biodegradable polymers.

2 Materials and testing methods

Natural Tussah or raw continuous long silkworm silk fibres and PLA granules were used in this study. Silk fibres were first chopped gently into short fibres with the length of 5 mm in which they were not stressed plastically during the fabrication process. 5, 10 and 15 vol % of short silk fibres were used to reinforce PLA to fabricate completely degradable composites. Before fabricating the composites, the silk fibres and PLA granules were first dried in an oven so as to remove excessive moisture. Composites were manufactured by injection moulding method to ensure consistent and reproducible products can be made. Silk fibres and PLA were fed into an injection moulding machine with injection barrel and mould pre-heated to the desired temperatures of 180 ^{o}C and 40 ^{o}C respectively. The mixture of fibres and PLA was left inside the injection barrel for 10 mins before injected so as to melt the PLA and mix with the fibres completely. These specific settings were optimised by orthogonal experiment with the consideration on the melting temperature of PLA and degradation temperature of silk fibre, as well as the Young's modulus and ultimate tensile strength of the composites under different settings of mixing time and temperature. Heat and pressure were added during the process in order to lower the viscosity of PLA to obtain a better permeability of resin into the fibres. Specific pressure and duration of each stage including the barrel, nozzle and injection mould were set to avoid shrinkage and air bubbles appeared in specimens. The first run of the injection was discarded and the resultant specimens were in the shapes of rods, bars, and waisted according to ASTM standards.

2.1 Mechanical property tests

Tensile property test was carried to examine the force-displacement relationship of neat PLA waisted specimens and 5, 10 and 15 vol % of silk/PLA composites by using a 500 N load cell and a scanning laser extensometer, and crosshead speed with a loading rate of 2 mm/min was set. Results of load and displacement of specimens under tension were recorded. Additionally, the ultrasonic resonance analyser is a non-destructive testing device, which can be used to determine the stiffness of materials. The specimens were made into rectangular bars and excited by a mechanical impulse. The resonant frequency of the excited specimen was recorded by a microphone. The Young's modulus of the material was then calculated with the weight, dimensions and Poisson's ratio of the specimen. Lastly, rod-shaped injection moulded specimens were used for Izod impact test to determine the toughness of neat PLA and silk/PLA specimens. A pendulum swung on its track and struck the plastic specimens. The resultant angles of the pendulum were recorded. The energy lost to break the specimen as the pedulum continued on its path was then measured from the distance of its follow through.

2.2 Fourier Transform Infrared Spectroscopy (FTIR)

FTIR is a powerful tool for protein conformation analysis thus it is widely used to study the molecular structure and reveals typical transmittance bands sensitive to molecular conformation of silk fibre. The band range between 2000 and 1000 cm^{-1} was selected for estimating the band assignments in the silk fibre. In addition, injection moulded neat PLA, 5, 10 and 15 vol% silk/PLA composite specimens were also tested by FTIR for band assignments comparison.

2.3 Microscopic Analysis

Optical microscope was used to examine the dispersion and orientation of fibres inside a composite specimen manufactured by injection moulding technique. Specimens in rectangular

shape were polished so as to expose the short silk fibres to the surface of the specimens. By making use of the microscopy software, pictures of different sections of the specimen were merged to show a full picture of the composite. Moreover, SEM was used on the fracture surfaces of specimens to examine their fracture surface structure and failure behaviour induced by the Izod impact tests.

3 Results and Discussion

By making use of conventional tensile testing technique with the help of a 500 N load cell and a scanning laser extensometer, comparison on peak load and strain at break of neat PLA specimens and silk/PLA composites is shown in Figure 1. In order to maintain the accuracy of measurement, all testing specimens were moulded into a waisted shape under the same conditions with the same dimensions. All specimens were broken in the waisted gauge span and the values obtained from the test with the help of the scanning laser extensometer show that the failure modes of each set of specimens can be considered as consistent. Average of 6 specimens in each set of material with different fibre content was taken.

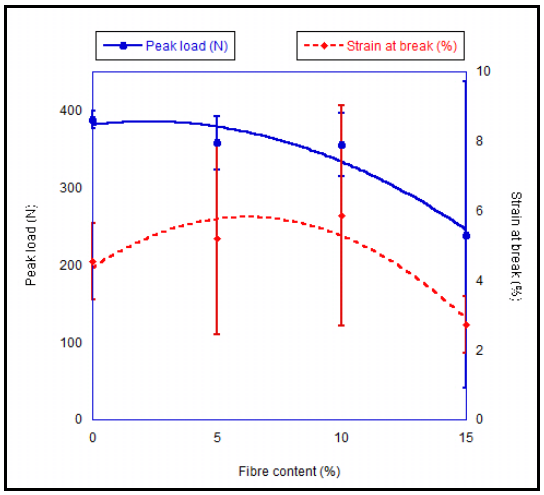

Figure 1 Peak load and strain at break against fibre content on neat PLA specimens and silk/PLA composites

Neat PLA specimen has a maximum load of 388 N and there is a decrement of 8 – 38 % of this value when the fibre content was increased from 5 to 15 vol% to the specimen respectively. On the other hand, there is an increment of strain at break to these specimens when the fibre content increased from 5 to 10 vol% of approximate 15 to 30 % to that of neat PLA specimens with 4.55 % strain at break. Short silk fibre reinforcement enhanced the ductility of the PLA matrix, at the same time, it decreased the maximum load that the material can sustain. Moreover, from both of the plots, it can be noted that the mechanical properties of the composite were weakened in both the strength and elongation when more than 10 vol% of silk fibres were reinforced.

Ultrasonic resonance analysis is a non-destructive testing technique, which can be used to determine the stiffness of materials. As seen in Figure 2, by altering the fibre content in the composite, the stiffness of the material has a significant change. Average of 6 specimens in each set of material with different composition was taken in this test. The Young's modulus of PLA was tested to be 3.7 GPa, with an increment of fibre content from 5 to 15 vol %, the Young's modulus was increased from 4 to 4.6 GPa, which is about 9 - 25 % increment compared to the neat PLA specimen.

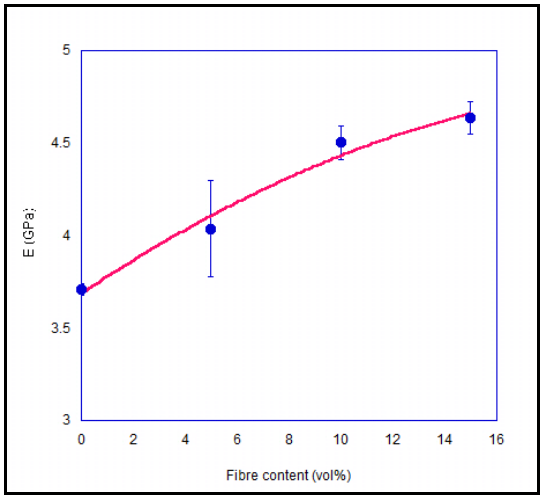

Figure 2 Young's modulus against fibre content of neat PLA specimens and 5 – 15 vol% silk/PLA composites

By Izod impact test, toughness of material as shown in Figure 3 can be determined. Average of 10 specimens in each set of material with different composition was taken in this test. As seen in the figure, there is an increase in fracture energy of the material with an increment of silk fibre content. The energy loss and fracture energy of neat PLA specimens are approximately 0.0020 J and 280 Jm^{-2} respectively, there is an about 70 % increment of both energy loss and fracture energy when 10 vol% of silk fibre was added to the composite. However, when more than 10 vol% of silk fibre was added to the composite, there is a significant drop of fracture energy, which is mainly due to the high volume percentage of fibre embedded in the matrix led to a weak interfacial bonding strength between fibre and matrix and this can be explained in SEM imaging.

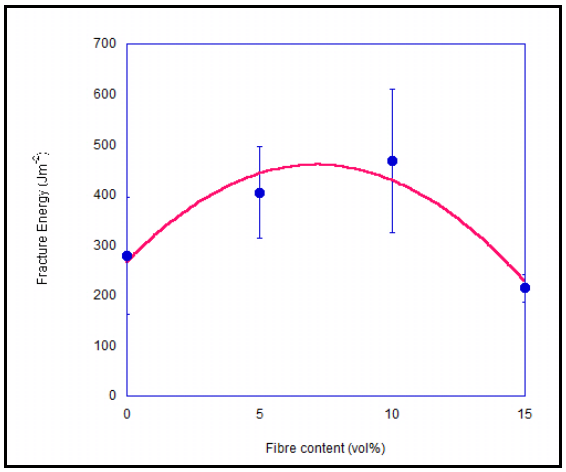

Figure 3 Fracture energy against fibre content of neat PLA specimens and 5 – 15 vol% silk/PLA composites

Therefore, according to the above mechanical property tests, by reinforcing natural Tussah silk fibres, the mechanical properties including ductility, stiffness and toughness of the biodegradable polymer PLA can be enhanced.

Generally speaking, there is a presence of α-helical, anti-parallel and parallel β-sheet, and random coil structures in the specific amide I, II and III regions of the study of silk protein spectrum by FTIR. All amides exhibit a band due to the C=O stretching vibration, with primary and secondary amides also having bands due to the N-H stretching and deformation vibrations. Amide I and II bands are major bands of protein infrared spectrum. The amide I band (1600 – 1700 cm^{-1}) is mainly associated with the C=O stretching vibration and directly related to the backbone conformation. Amide II (1510 – 1580 cm^{-1}) is attributed from the N-H bending vibration and the C-N stretching vibration. Moreover, the N-H bands are dependent to the amount of hydrogen bonding occurring. In Figure 4a, the spectrum of silk fibre is characterised by the transmittance bands at 1620 cm^{-1} (medium - strong intensity, amide I band), 1516 cm^{-1} (strong intensity, amide II band) and 1234 cm^{-1} (medium intensity, amide III band). The amide I band at 1620 cm^{-1} can be assigned to side chains or aggregated strands with strong intermolecular hydrogen bonds among the β-sheet. The peaks at amide II (1516 cm^{-1}) and amide III (1234 cm^{-1}) are attributed to β-sheet conformation [7-14]. In Figure 4b, a comparison on FTIR spectrum of neat PLA specimen and different fibre content silk/PLA composites was made. For neat PLA specimen, there are peaks at 1749 cm^{-1} (very strong intensity, C=O stretching), 1452 cm^{-1} (medium intensity, asymmetric bending deformation of CH_3), 1383 cm^{-1} and 1358 cm^{-1} (medium - strong intensity, symmetric deformation of CH_3), 1265 cm^{-1}, 1180 cm^{-1} and 1084 cm^{-1} (strong intensity, asymmetric and asymmetric C-O-C stretch) [15-17]. By comparing silk/PLA composites with different fibre content to that of the silk fibre and neat PLA specimen in Figure 4a and b, it can be seen that by increasing the fibre content in composite, all the band assignments of PLA decrease in transmittance magnitude. When 10 and 15 vol% silk fibres were used to reinforce PLA, the composites show a significant combination of band assignments of neat PLA and silk fibre in the results at bands 1620 and 1516 cm^{-1}. That is to say, higher silk fibre content reinforcement does affect the molecular structure and molecular conformation of PLA.

a. b.

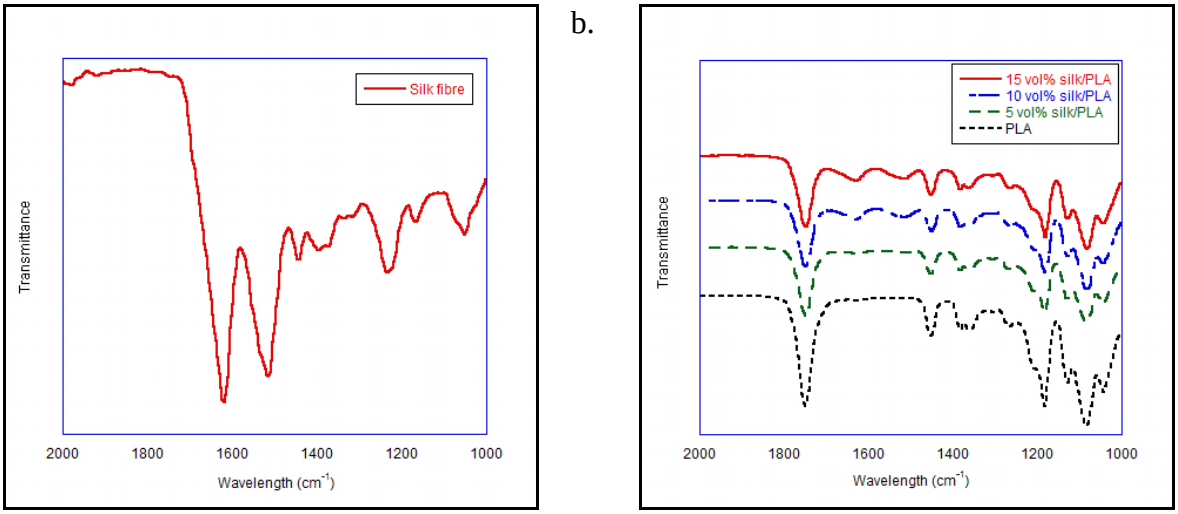

Figure 4 FTIR plots of a. silk fibre, and b. neat PLA specimen and 5 – 15 vol% silk/PLA composites

Short fibre-reinforced composites usually have problems on fibre dispersion and orientation. By using injection moulding technique in making specimens, consistency and reproducibility of specimens can be maintained. On the other hand, fibre dispersion and orientation inside the composite can be determined by merging the optical microscopy images as shown in Figure 5.

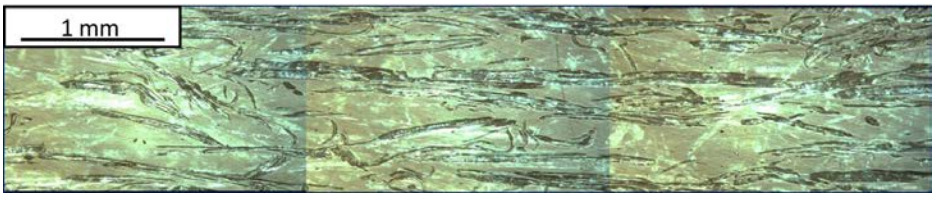

Figure 5 Optical microscopy image on 10 vol% silk/PLA composite

It can be seen in the figure that the majority of fibres in the composite are aligned and dispersed along the axial direction of the composite, which is due to the polymer flow direction during injection moulding of specimen. With respect to the dimension of fibres, it shows that the diameter of the short fibres varies. Silk fibres are in lengthwise striation but with highly non-uniform cross-sectional geometry from sections to sections along one single fibre, which is generally due to different species of silkworms, and the surrounding environment and situation when the silk fibres were produced and reeled. Moreover, according to previous studies on silk fibre composites, fibres form micro-pins and mesh-like structure inside the composite when molten polymer permeates into the fibre filaments, thus some of the fibre filaments cannot be seen on the surface of the specimen by optical microscopy imaging.

In order to comprehensively investigate the root cause of failure and fibre-reinforced mechanisms of the composites, a study on their failure patterns and mechanisms is essential. Neat PLA and 5 - 15 vol% silk/PLA composite specimens after conducting Izod impact test were cut into small pieces for microscopic investigation through SEM imaging in Figure 6a - d.

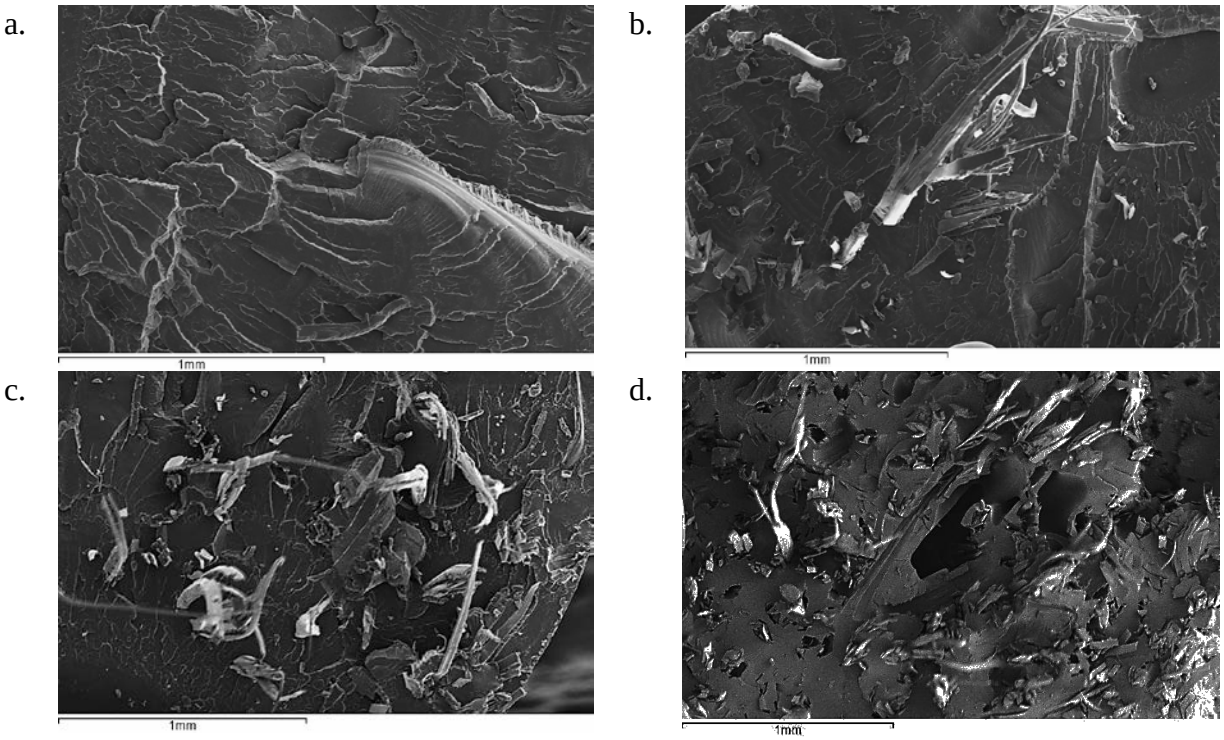

Figure 6 SEM images on fractured specimen surfaces a. neat PLA; b. 5 vol% silk/PLA; c. 10 vol% silk/PLA; d. 15 vol% silk/PLA

Based on previous studies, it is found that the control of manufacturing process of silk-based polymer composites is a crucial factor to produce high strength and reliable composites. The purpose of adding heat and pressure to the materials during the injection moulding process is to lower the viscosity of the polymer and thus increase its permeability into the core of fibroin filaments in silk fibres, which in turn to enhance the interfacial bonding properties between the polymer and fibres. There is no doubt that the mechanical performance of fibre-reinforced composites is mainly governed by the stress transferability between fibres and matrix. The amount of surface contact between the fibre and matrix is the first key, and the bonding action between them is another key issue. Consequently, high permeability of polymer into the fibres can improve the total contact surface area and interfacial bonding between reinforcements and matrix in the composites. Conversely, when high silk fibre content was used to reinforce PLA, i.e. 15 vol%, the permeability of polymer into fibres would be difficult, interfacial bonding strength between fibres and matrix was then weakened and fibres were easily pulled out from the matrix, thus the mechanical properties of the composite were decreased.

4 Conclusions

Injection moulded neat PLA and 5 - 15 vol% silkworm silk/PLA composites were under investigation. For mechanical property testing, the ductility, stiffness and toughness of PLA were enhanced with 5 - 10 vol% silk reinforcement. There is a drop in mechanical properties of the material when high fibre content was used as reinforcement and can be claimed as the weak interfacial bonding between fibres and matrix induced by high fibre volume. Fibres were dispersed and aligned inside the composite. Lastly, chemical characterisation by FTIR determined the combination effect on silk/PLA composite when different fibre content was used.

References

[1] Mohanty A.K., Misra M., and Hinrichsen G.. Biofibres, biodegradable polymers and biocomposites: An overview. *Macromolecular Materials and Engineering*, **276**(3-4), pp. 1-24 (2000).

[2] Cheung H.Y., Lau K.T., Tao X.M. and Hui D.. A potential material for tissue engineering: Silkworm silk/PLA biocomposite. *Composites Part B: Engineering*, **39**(6),pp1026-1033 (2008).

[3] Altman G.H., Diaz F., Jakuba C., Calabro T., Horan R.L., Chen J., Lu H., Richmond J. and Kaplan D.L.. Silk-based biomaterials. *Biomaterials*, **24**(3),pp 401-416 (2003).

[4] Vepari C. and Kaplan D.L.. Silk as a biomaterial. *Progress in Polymer Science*, **32**(8-9), pp 991-1007 (2007)

[5] Sun X.S., ed. *Plastics derived from starch and poly(lactic acids)* in "Bio-based polymers and composites", edited by Wool R.P. and Sun X.S., Elsevier Academic Press, U.K. (2005).

[6] Karnani R., Krishnan M. and Narayan R.. Biofiber-reinforced polypropylene composites. *Polymer Engineering and Science*, **37**(2), pp 476-483 (1997).

[7] Prasong S., Yaowalak S. and Wilaiwan S.. Characteristics of silk fiber with and without sericin component: a comparison between Bombyx mori and Philosamia ricini silks. *Pakistan Journal of Biological Sciences*, **12**(11), pp 872-876 (2009).

[8] Khan M.M.I.R., Morikawa H., Gotoh Y., Miura M., Ming Z., Sata Y. and Iwasa M.. Structural characteristics and properties of Bombyx mori silk fiber obtained by different artificial forcibly silking speeds. *International Journal of Biological Macromolecules*, **42**(3), pp 264-270 (2008).

[9] Ayub Z.H., Arai M. and Hirabayashi K.. Quantitative Structural-Analysis and Physical-Properties of Silk Fibroin Hydrogels. *Polymer*, **35**(10), pp 2197-2200 (1994).
[10] Chang J.C., Gurr G.M., Fletcher M.J. and Gilbert R.G.. Structure-property and structure-function relations of leafhopper (Kahaono Montana) silk. *Australian Journal of Chemistry*, **59**(8), pp 579-585 (2006).
[11] Test report for Avesta 17-11-2 L (0.4 mm sheet). Avesta Polarit AB prinox: Langshyttan (2003).
[12] He J.X., Qin Y.R., Cui S.Z., Gao Y.Y. and Wang S.Y,. Structure and properties of novel electrospun tussah silk fibroin/poly(lactic acid) composite nanofibers. *Journal of Materials Science*, **46**(9), pp 2938-2946 (2011).
[13] Taddei P., Monti P., Freddi G., Arai T. and Tsukada M.. IR study on the binding mode of metal cations to chemically modified Bombyx mori and Tussah silk fibers. *Journal of Molecular Structure*, **651**, pp 433-441 (2003).
[14] Shao J.Z., Zheng J.H., Liu J.Q. and Carr C.M.. Fourier transform Raman and Fourier Transform infrared spectroscopy studies of silk fibroin, *Journal of Applied Polymer Science*, **96**(6), pp 1999-2004 (2005).
[15] Krikorian V. and Pochan D.J.. Crystallization behavior of poly(L-lactic acid) nanocomposites: nucleation and growth probed by infrared spectroscopy. *Macromolecules*, **38**, pp 6520-6527 (2005).
[16] Freddi G., Monti P., Nagura M., Gotoh Y. and Tsukada M.. Structure and molecular conformation of tussah silk fibroin films: effect of heat treatment. *Journal of Polymer Science Part B: Polymer Physics*, **35**(5), pp 841-847 (1997).
[17] Socrates G.. *Infrared Characteristic Group Frequencies Tables and Charts 2nd Ed.*. John Wiley & Sons, U.K. (1994).